

Performance of Contactless Micro Vibration Isolator Using Flux Pinning Effect

By Takuma SHIBATA,¹⁾ and Shin-ichiro SAKAI²⁾

¹⁾*Department of Aerospace and Astronautics Science, SOKENDAI, Kanagawa, Japan*

²⁾*Institute of Space and Astronautical Science, JAXA, Sagamihara, Japan*

(Received June 21st, 2017)

Exploring planets and Galaxies gives us information about space. Space telescopes have been used for acquiring information about the planets and galaxies which are far from the Earth. NASA has been developing the James Webb Space Telescope with a pointing accuracy requirement higher than that of conventional telescopes to get high resolution data of a target. To achieve this pointing objective, the influence of heat and vibration must be paid attention. The micro vibration isolator utilizing the flux pinning effect is proposed to resolve those challenging problems for next generation space telescopes. A mission part and a bus part are connected using the flux pinning effect. The effect is yielded between a type-II superconductor and a material generating magnetic flux. An initial relative distance and attitude between those materials are maintained without control due to retentive forces called pinning force. The initial values are decided when the type-II superconductor is cooled below a critical temperature. The pinning force can be approximated by linear spring-damping force, therefore those properties are adapted to the micro vibration isolator. The proposed isolator is mainly composed of type-II superconductors, permanent magnets, metal plates and magnetic coils. The isolator can change the observation direction with an infinitesimal angle by controlling magnetic flux from magnetic coils. Performance of the proposed isolator is evaluated and discussed in this paper. To understand the performance, the frozen image model, which is validated by an experiment, is used.

Key Words: Micro vibration isolator, Flux pinning effect, Formation flight

Nomenclature

ω	:	Natural frequency
ζ	:	Damping ratio
k	:	Spring coefficient
c	:	Damping coefficient
W	:	Mass
M	:	Magnetic moment
r	:	Position
F	:	Force
T	:	Torque
μ_0	:	Permeability
R	:	Radius
H	:	Height
A	:	Area
Subscripts		
mis	:	Mission part
bus	:	Bus part
f	:	Frozen image
m	:	Mobile image
p	:	Pinning force
fc	:	Field Cooling
sp	:	Sun Pressure
pe	:	Permanent Magnet

1. Introduction

High pointing accuracy for observing a target which is far from the Earth is a requirement for space telescopes. In order to achieve this requirement, the influence of heat and vibration on the mission part must be cared. Actuation components such as the reaction wheel and cryocooler in the bus part and solar radiation are considered as sources for thermal disturbances. These

disturbances must be attenuated for observing a target with high pointing accuracy. A mission part of the SPICA which will be launched in 2027 should be cooled to 8 K to discover an exoplanet¹⁾. The James Webb Space Telescope is being developed by NASA and will be launched in 2018. The Mid-Infrared Instrument (MIRI) in the mission part must be cooled down to approximately 6 K²⁾. As a solution for thermal problem, a thermal shield has been equipped between the mission and bus parts. Actuators in the bus part generate not only heat but also vibration which is one of the factor reducing the pointing accuracy. As the vibration transmits to the mission part, observed data gets blurred.

Conventional methods to suppress the vibration have been applied for space telescopes. Stewart Gough Platform (SGP) has been studied for this purpose³⁾⁻⁶⁾. SGP is composed of movable struts which have spring damping characteristic and those struts can be controlled to suppress the influence of vibration with 6 DOF. The control method to suppress the vibration is presented for stabilizing resolution of observed scientific data using SGP³⁾. The effectiveness is demonstrated not only with the simulations but also with an experiment. D-strut developed by Honeywell has been also utilized as a vibration isolator for a space telescope and is utilized as movable struts in SGP⁴⁾. Three types hexapod geometries using voice coil motors is investigated for SGP⁵⁾. SGP that uses flexible joint and magnetic-voice coil actuator with skyhook damper is proposed⁶⁾. This method improves the vibration characteristics of conventional SGP.

As other methods, Tip Tilt Mirror(TTM) is also an effective method and has been used for space telescopes⁷⁾. Actually TTM was mounted on Sclar-B and contributed for acquiring data about magnetic field of the Sun⁸⁾.

In the case of using a vibration isolator like SGP or D-strut,

which connects the mission and bus parts mechanically, heat generated by the bus part transmits to the mission part through the vibration isolator. A method to solve these thermal and vibration problems at same time is proposed by Lockheed Martin. The vibration isolator, which is called as Disturbance-Free Payload (DFP)⁹⁾, does not require mechanical connection between the bus and mission parts. As there is no connection, the influence of heat transferring through the vibration isolator can be suppressed. This isolator uses electro-magnetic coil to maintain the relative distance and attitude between the mission and bus parts. In addition, the mission and bus parts of the spacecraft that uses DFP can be constructed separately since two parts are not structurally connected. Thus space telescopes building time shortens.

The flux pinning effect is applied to a micro vibration isolator(Fig.1)¹⁰⁾. The flux pinning effect enables maintaining the relative distance and attitude between a type-II superconductor and a material generating magnetic flux without an actuator. When a superconductor is cooled below the critical temperature, then the conducting state, which does not have any special effect, is changed to superconducting state. In superconducting state, the type-II superconductor has two special effects, which are called as the perfect diamagnetism and the perfect conductivity.

Usually external magnetic field can not intrude in a superconductor which is in superconducting state by the perfect diamagnetism, which is also called the Meissner effect. However, in case of a type-II superconductor, where the external magnetic field that exceeds the lower critical magnetic field applies to the type-II superconductor, the magnetic flux intrudes and is pinned in the type-II superconductor. In addition, the field cooling method is also an effective method to form the flux pinning effect. In this method the external magnetic field applies to a type-II superconductor, which is in normal conducting state, and then the type-II superconductor is cooled below the critical temperature. Using this method, the equilibrium point can be decided. Relative distance and attitude are maintained by retentive force called as the pinning force even if disturbance affects. This pinning force can be approximated by linear spring damping force with infinitesimal displacement, so those characteristics are applied to suppress the influence of micro vibration without actuator.

In section 2, technologies using the flux pinning effect are introduced and then the proposed micro vibration isolator is illustrated. The proposed isolator configuration is introduced and

frequency characteristics for the proposed isolator are indicated. In section 3, a numerical calculation model based on the frozen image model is indicated. The calculation model for the proposed isolator which is formed of few permanent magnets is indicated. The spring coefficient, which has a relation with the radius of a permanent magnet and initial relative distance between the mission and bus parts, is also derived. On Halo orbit at Sun-Earth L2 point, solar pressure is dominant, hence solar pressure disturbance are calculated in section 4 and compared with the pinning force and torque in next section. In section 5, numerical results are indicated to understand the properties of the proposed isolator. In case that the proposed isolator is required to suppress broadband vibration, low spring coefficient is desirable. Then the pinning force becomes small. Those characteristics of the force and torque are compared with disturbance force and torque.

2. Flux-pinned Micro Vibration Isolator

2.1. Space technologies using flux pinning effect

The relative motion between a type-II superconductor and a permanent magnet is fixed in space using the flux pinning effect. Thus formation flight techniques using the flux pinning effect have been researched. This formation flight technology using the flux pinning effect has robustness in autonomous operations because the flux pinning effect can maintain the relative position without an active control. The satellite in formation can change the position using magnetic coils¹¹⁾¹²⁾. This allows the shape of the formation to change to a form which is advantageous for the mission or motion of the formation.

Rendezvous docking using the flux pinning effect has also been considered¹³⁾. Rendezvous docking using a robot arm is used to dock each spacecraft to the International Space Station (ISS). The rendezvous docking system using the flux pinned interface (FPI) has been researched for autonomous rendezvous docking. NASA/JPL is looking at a Martian sample return mission in MARS2020¹⁴⁾¹⁵⁾. In this mission, a Mars rover gathered by a Mars rover will be launched to the orbit and an explorer will fetch the sample return capsule before returning to the Earth. The flux pinning effect is considered for rendezvous docking system to fetch the sample capsule.

2.2. Flux-pinned micro vibration isolator configuration

The flux pinning effect is utilized for a micro vibration isolator which does not require any control for suppressing the influence of the vibration and maintaining the relative distance and attitude. The mission and bus parts of a spacecraft that has Flux-pinned Micro Vibration Isolator (FMVI) are connected not mechanically but electro-magnetically. FMVI is composed of few type-II superconductors, permanent magnets, eddy current dampers and magnetic coils as in Fig.2 . The flux pinning effect can maintain the relative distance and attitude between a cooled type-II superconductor and a permanent magnet passively as a result of the pinning force. The pinning force can be approximated by linear spring damping force. Type-II superconductors must be cooled below the critical temperature, which is 93K with YBCO material, to maintain the pinning force. A spacecraft such as the SPICA or the JWST can cool the mission part below the critical temperature sufficiently using a sunshield and a cryocooler. It assumes that FMVI is mounted on one of

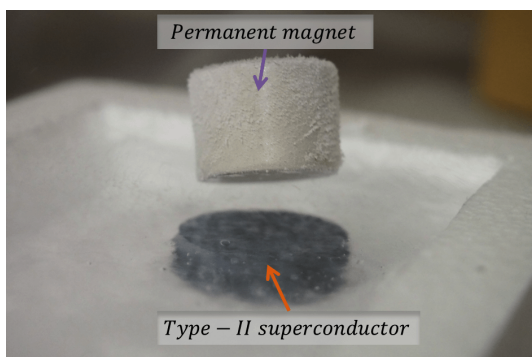


Fig. 1. Flux pinning effect

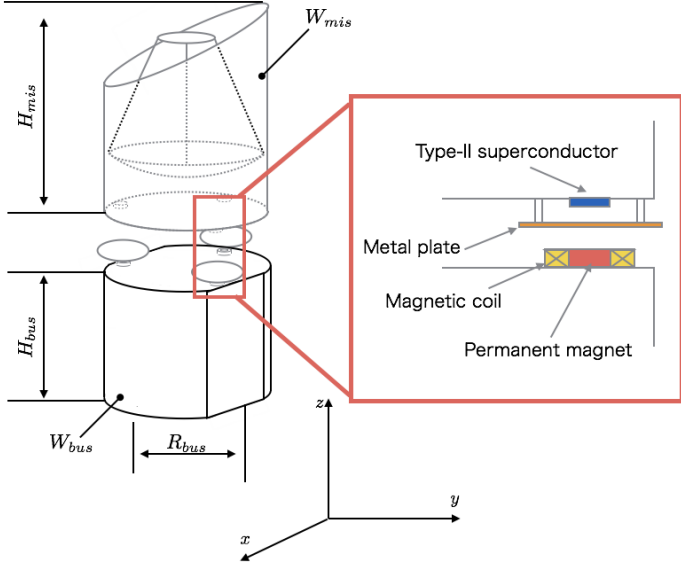


Fig. 2. Proposed isolator

these spacecraft, hence type-II superconductors are mounted on the mission part. It is well known that damping force by the flux pinning effect is weak¹⁶⁾¹⁷⁾, so the eddy current damper is applied to the isolator to improve the vibration characteristics. Magnetic coils are mounted on each part and used to prevent dangerous phase which is represented by separation of each part. These magnetic coils are used to maintain the relative distance and attitude such as Electro-Magnetic Formation Flight (EMFF) in dangerous situation¹⁸⁾. In addition, those electro-magnetic coils are used for adjustment of the observation direction. Repulsive force occurs between external magnetic flux and a cooled type-II superconductor by the perfect diamagnetism. Therefore, controlling magnetic field generated by these magnetic coils can be used for changing the observation direction with infinitesimal angle. This adjustment using the electro-magnetic coils can be useful for a space telescope that observes a distant target. It supposes that the space telescope having FMVI performs a mission on Halo orbit at Sun-Earth L2 point.

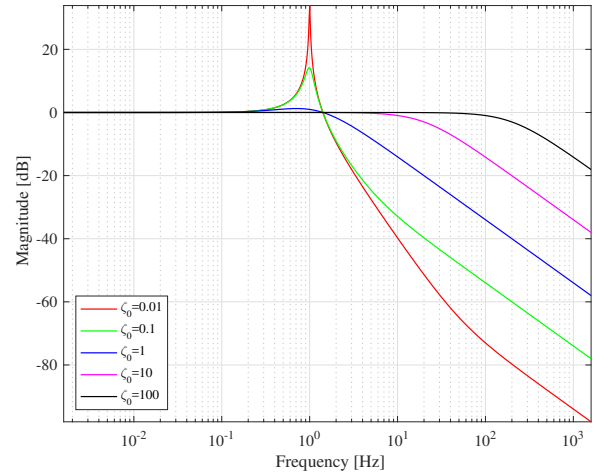
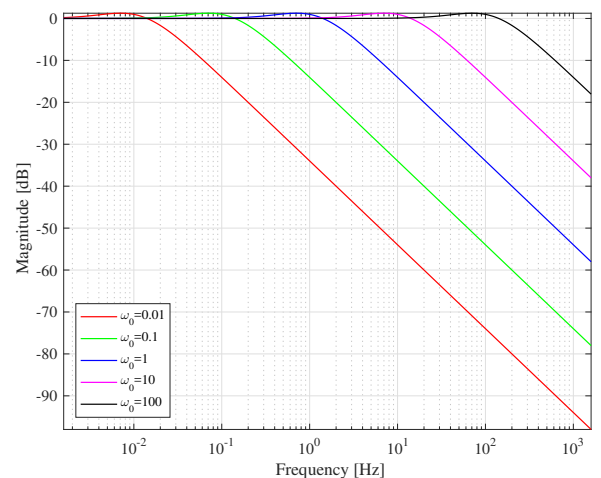
To suppress the vibration in broadband, spring coefficient have to be small and damping coefficient is adjusted to prevent resonance in a linear spring damping system. The frequency characteristics can be written by natural frequency ω_n and damping ratio ζ_n as a linear spring damping system is considered. Natural frequency and damping coefficient is expressed by spring coefficient k , damping coefficient c and mass W :

$$\omega_n = \sqrt{\frac{k}{W}}, \quad (1)$$

$$\zeta_n = \frac{c}{2\sqrt{Wk}}. \quad (2)$$

When only vertical vibration is considered, which is along with z axis, then the equation of motion can be written as

$$\begin{cases} W\ddot{z} + c\dot{z} + kz = u \\ p = c\dot{z} + kz. \end{cases} \quad (3)$$

Fig. 3. Frequency response between force input and force output as damping ratio is changed with natural frequency $\omega_n = 1$ Fig. 4. Frequency response between force input and force output as natural frequency is changed with damping ratio $\zeta_n = 1$

Transfer function $H(s)$ between force input and force output can be derived from the Laplace transformed equation of motion:

$$H(s) = \frac{P(s)}{U(s)} = \frac{2\omega_n\zeta + \omega_n^2}{s^2 + 2\omega_n\zeta s + \omega_n^2}. \quad (4)$$

The frequency response characteristics are shown in Fig.3 and Fig.4 as $W = 1kg$. As seen in Fig.3, damping ratio affects to suppress the resonance however cut-off frequency moves to high frequency when damping ratio becomes higher than $\zeta_n = 1$.

In Fig.4, when natural frequency is small, cut-off frequency move to low frequency band. Natural frequency ω_n is depending on spring coefficient k and mass W . Hence it may be changed by designing the spring coefficient and mass. To suppress the broadband vibration, natural frequency must be small. From these results, the micro vibration isolator, which can suppress the vibration passively, requires a low spring coefficient and a damping coefficient that is designed to suppress the resonance.

Damping force of the flux pinning effect is small, therefore the eddy current damper is inserted between a permanent

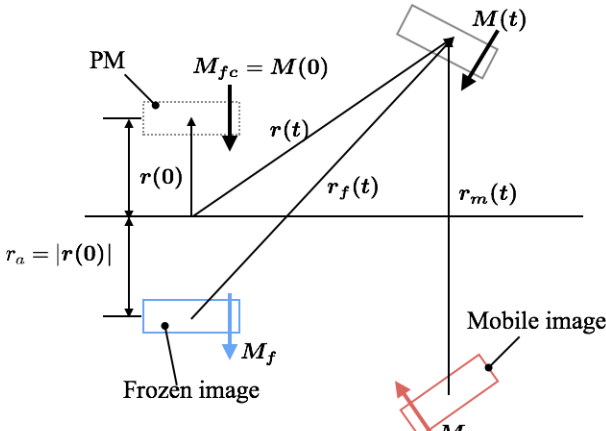


Fig. 5. Frozen image model

magnet and a type-II superconductor in the proposed isolator. Damping force by the eddy current damper can be changed by varying the design specifications for the metal.

3. Numerical calculation model

3.1. Frozen image model

The frozen image model¹⁹⁾ is applied to understand simply the properties of FMVI. It considers that the pinning force is affecting between a type-II superconductor and a permanent magnet and the permanent magnet is modeled as magnetic dipole in this paper. The type-II superconductor is sufficiently large compared with the permanent magnet and made of an ideal material as in Fig.5. The relative position between the permanent magnet and the type-II superconductor is pinned by the flux pinning effect and this position can be decided using field cooling method. The retentive force and torque increases by deviation from the initial point at field cooling.

In frozen image model, two types of image, which are called the frozen image and the mobile image, are used for estimating the force and torque by the flux pinning effect. Those images have same magnetization with a material which magnetic flux is pinned in the type-II superconductor. The magnitude of magnetization is decided when the field cooling method is applied. The relation of magnetic moment vectors is $|M_{fc}| = |M_f| = |M_m|$, where M_{fc} is the magnetic moment vector of the permanent magnet at the field cooling and M_f and M_m are the magnetic moment vector of the frozen image and the mobile image, respectively. The magnetic moment vector and position of the frozen image are decided during the field cooling and not changed even if the permanent magnet is moved from the initial position. In contrast, the mobile image's magnetic moment vector and position are changed by the position of the permanent magnet from the initial point.

The frozen image model is an effective model for estimating the force and torque by the flux pinning effect, however dynamics depending on relative motion can not be calculated. Therefore, this model does not take the damping force into account. Damping effect by the eddy current damper is stronger than that of the flux pinning effect, therefore the damping force is estimated by calculating the eddy current on a metal plate for the proposed isolator. The magnetization vector of the permanent magnet during the field cooling is defined as M_{fc} and

regarded as magnetic dipole. Then these relationships can be expressed¹³⁾

$$M_f = 2(\mathbf{a} \cdot M_{fc})\mathbf{a} - M_{fc}, \quad (5)$$

$$M_m = M - 2(\mathbf{a} \cdot M)\mathbf{a}. \quad (6)$$

M is the magnetization vector of the permanent magnet which moves from the initial point. The magnetization vector changes in time if an external force applies between these materials. The position vector of the frozen and mobile image on Cartesian coordinate system r_f and r_m can be expressed as

$$r_f = \mathbf{r} - \mathbf{r}_{fc} + 2(\mathbf{a} \cdot \mathbf{r}_{fc})\mathbf{a}, \quad (7)$$

$$r_m = 2(\mathbf{a} \cdot \mathbf{r})\mathbf{a}, \quad (8)$$

where \mathbf{a} is an unit vector and defined as perpendicular on type-II superconductor's surface as $\mathbf{a} = [0, 0, 1]$. A point which is on the surface of the type-II superconductor is defined, then $\mathbf{r}(t)$ is expressed as a position vector which is from the point to the levitated permanent magnet. \mathbf{r}_{fc} is a position vector at the field cooling and is constant with $\mathbf{r}_{fc} = \mathbf{r}(0)$.

In this model, the magnetization vector and position of the frozen image model are decided during the field cooling. The magnetic force and torque affect between two images and the levitating permanent magnet and can be calculated as

$$\mathbf{F}_{f,m} = \nabla H_{f,m} \cdot \mathbf{M}(t), \quad (9)$$

$$\mathbf{T}_{f,m} = \mathbf{M}(t) \times \mathbf{H}_{f,m}. \quad (10)$$

Finally, the pinning force and torque generated by changing magnetic field can be denoted as,

$$\mathbf{F}_p = \mathbf{F}_f + \mathbf{F}_m, \quad (11)$$

$$\mathbf{T}_p = \mathbf{T}_f + \mathbf{T}_m. \quad (12)$$

Here, it is considered that the force and torque affect between multiple permanent magnets and type-II superconductors by flux pinning effect. Magnets and type-II superconductors are located at the vertexes of a regular N-sided polygon. A type-II superconductor and all permanent magnets are connected magnetically by the flux pinning effect. Namely the frozen image and mobile image are generated by each permanent magnet PM in a type-II superconductor SC and those images affect other permanent magnets. Those PM and SC are given a number with clockwise order from PM_1 which is on x axis as in Fig.6. Let FI_l and MI_l be the frozen image and mobile image which are generated by PM_l during the field cooling in the type-II superconductor SC_l . Relative position vector from each images to a permanent magnet is expressed as

$$\mathbf{r}_{f(p,q)} = \mathbf{r}_q - \mathbf{r}_{fc_q} + 2(\mathbf{r}_{fc_q} \cdot \mathbf{a})\mathbf{a} + (\mathbf{r}_{fc_q} - \mathbf{r}_{fc_p}), \quad (13)$$

$$\mathbf{r}_{m(p,q)} = 2(\mathbf{r}_q \cdot \mathbf{a})\mathbf{a} + (\mathbf{r}_{fc_q} - \mathbf{r}_{fc_p}). \quad (14)$$

Then, the subscription p indicates a number of an image in SC_p and the subscription q means a number of a permanent magnet PM_q . Finally, the pinning force and torque affecting between the mission and bus parts for the proposed isolator with multiple permanent magnets are derived as:

$$\mathbf{F}_{np} = \sum_{p=1}^n \sum_{q=1}^n \mathbf{F}_f(\mathbf{r}_{f(p,q)}) + \sum_{p=1}^n \sum_{q=1}^n \mathbf{F}_m(\mathbf{r}_{m(p,q)}), \quad (15)$$

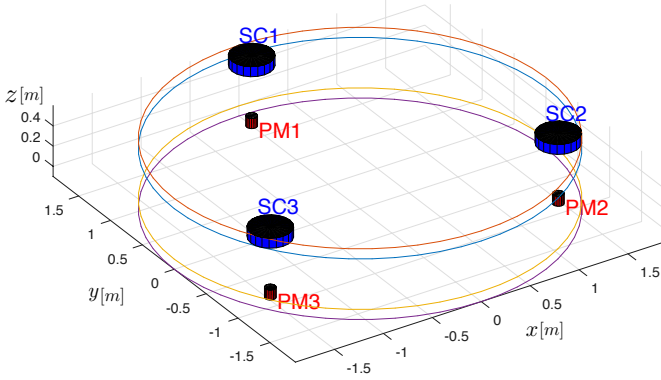


Fig. 6. Position of three permanent magnets and type-II superconductors on each part

$$\mathbf{T}_{np} = \sum_{p=1}^n \sum_{q=1}^n \mathbf{T}_f(\mathbf{r}_{f(p,q)}) + \sum_{p=1}^n \sum_{q=1}^n \mathbf{T}_m(\mathbf{r}_{m(p,q)}). \quad (16)$$

In this paper, it assumes that the proposed isolator is composed of three sets ($n=3$) of a permanent magnet and a type-II superconductor as in Fig.6. Small spring coefficient is required to suppress the vibration in broadband. To design the proposed isolator, spring coefficient related to radius of a permanent magnet and relative distance between a mission part and a bus part is expressed. Since these permanent magnets and superconductors are affecting each other in this proposed isolator, it is difficult to derive the relation between the pinning force, size of a permanent magnet and initial relative distance analytically. Thus the relation between $\{\mathbf{F}_{p_{di}} = \mathbf{F}_{np(p,q)} | p = q\}$ and $\{\mathbf{F}_{p_{indi}} = \mathbf{F}_{np(p,q)} | p \neq q\}$ is supposed and $\mathbf{F}_{p_{di}} \gg \mathbf{F}_{p_{indi}}$ is assumed. This assumption is used for the case that permanent magnets are put on the brink of a bus part and the radii is smaller than that of the bus part. Then, vertical pinning force along z axis F_{npz} , which affects between three permanent magnets and type-II superconductors ($n=3$), can be easily expressed as follows using this assumption:²⁰⁾

$$F_{3pz} = \frac{9\mu_0 M_z^2}{2\pi} \left[\frac{1}{(2(z_i + z))^4} - \frac{1}{(2z_i + z)^4} \right]. \quad (17)$$

$M_z = R_p^2 \pi H_p m_z$ is the magnetic moment of the permanent magnet and μ_0 is permeability. R_p and H_p are radius and height of the permanent magnet, respectively. m_z is the magnetization and the value was measured by the experiment.¹⁰⁾ Spring coefficient can be derived by differentiating F_{npz} :

$$k_{3pz} = \frac{18\mu_0 M_z^2}{\pi} \left\{ \frac{2}{(2z_i + 2z)^5} - \frac{1}{(2z_i + z)^5} \right\}. \quad (18)$$

Then, spring coefficient k'_{pz} at initial point $z = 0$ is

$$k'_{3pz} = \frac{9\mu_0 M_z^2}{16\pi z_i^5}. \quad (19)$$

Fig.7 indicates the relation between the radius of the permanent magnet R_p , the spring coefficient k'_{npz} , and the initial relative distance z_i . To achieve low spring coefficient, a small permanent magnet and large relative distance are required. R_p and H_p are set as 0.05[m] and assumed as constant in this paper. Then, spring coefficient at the initial point depends on the initial

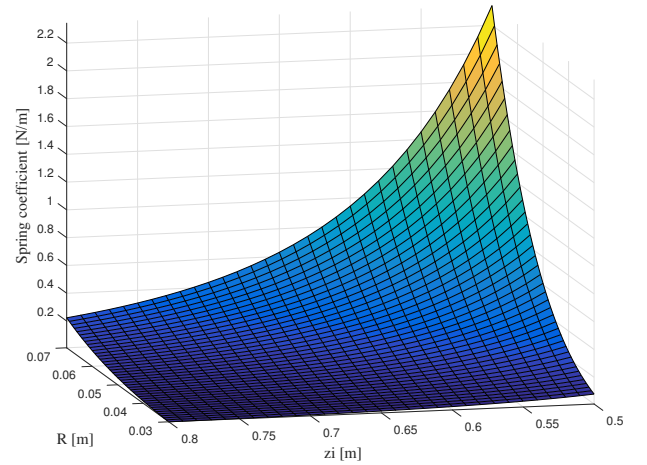


Fig. 7. Spring coefficient at initial point

relative distance between the permanent magnet and the type-II superconductor. In this paper, the initial relative distance is decided by Eq.(19) and the pinning force and torque are calculated. These force and torque are compared with disturbances for at orbit at Sun-Earth L2 point.

4. Disturbance model

4.1. Solar radiation pressure

Solar radiation pressure (SRP) is dominant on Halo orbit at L2 point for Sun-Earth system and the disturbance force and torque can be easily estimated by²¹⁾

$$F_{sp} = P_s A_m (1+q) \cos(i), \quad (20)$$

$$T_{sp} = P_s A_m H_m (1+q) \cos(i). \quad (21)$$

P_s is a solar radiation coefficient and its value is $4.617 \times 10^{-6} [\text{N}/\text{m}^2]$. A_m is the effective area of a space telescope. H_m is the length between the center of gravity and the point of sun pressure. q is the reflection coefficient and i is the angle between the effective area and the direction of Solar pressure. The maximum disturbance torque and force can be estimated by substituting the values as $q = 1$ and $i = 0^\circ$.

The maximum force by SRP is calculated using difference of effective area between the mission and bus parts:

$$A_m = 2|H_{mis}R_{mis} - H_{bus}R_{bus}|. \quad (22)$$

The maximum torque is calculated supposing that only the mission part rotates around the center of the mass. It is assumed that the center of mass is located on bottom of the mission part and SRP focuses on the top of the mission part. Then the length H_{mis} is substituted for H_m in Eq.(21). The space telescope configuration is assumed as in Table 1. In this case, the force and torque by SRP are calculated as 1.19×10^{-4} [N], 1.26×10^{-3} [Nm], respectively. However this influence can be decreased using a sunshield. When the sunshield activates, the mission part must be cooled for maintaining superconducting state of type-II superconductor. Therefore, to apply the sunshield to the space telescope that has FMVI is effective and this disturbance can be suppressed. In this paper, calculated SRP is regarded as one of the criterion for the pinning force and torque.

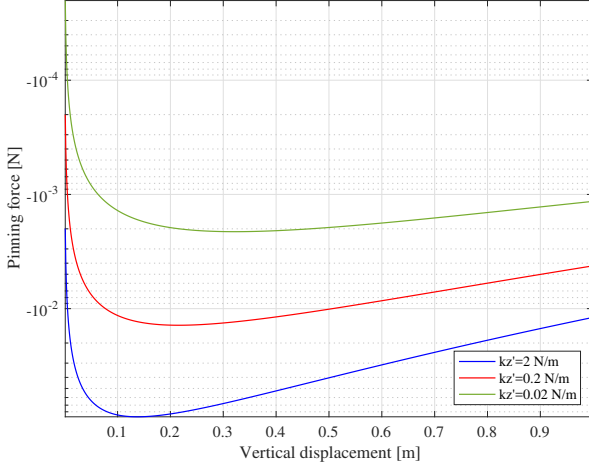


Fig. 8. The vertical pinning force when the position changes along with z axis

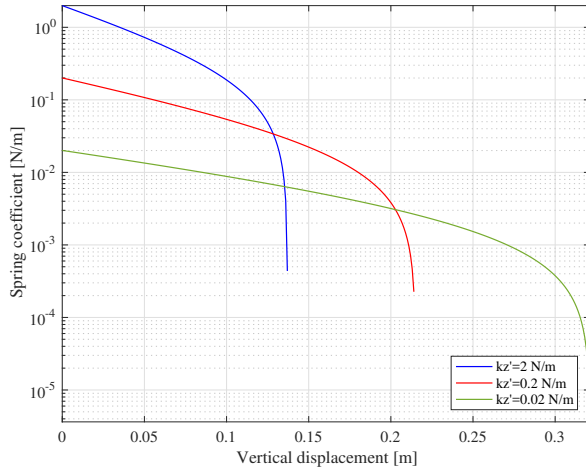


Fig. 9. The vertical spring coefficient when the position changes along with z axis

5. Results

The configuration of the space telescope and materials, which are the permanent magnets and the type-II superconductors, for the proposed isolator are assumed as in Table 1. In this paper, the size of the type-II superconductor is constant and assumed as an ideal material for the frozen image model. Fig. 8 and Fig. 9 show the vertical pinning force and the vertical spring coefficient respectively when the position changes along with the vertical axis. k'_z means the vertical spring coefficient at the initial point in these results.

As seen in these results, as the vertical spring coefficient k'_z decreases the pinning force decreases. The low spring coefficient is required for suppressing the influence of vibration in broadband, however the pinning force also decreases significantly. This leads the results that the space telescope is broken up. Magnetic coils on our proposed isolator are used to maintain the relative distance by compulsion for the accident.

However the vertical spring coefficient $k'_z = 0.02 \text{ N/m}$ is the limitation when the pinning force is compared with SRP in the space telescope configuration. As seen in Fig. 9, there are fi-

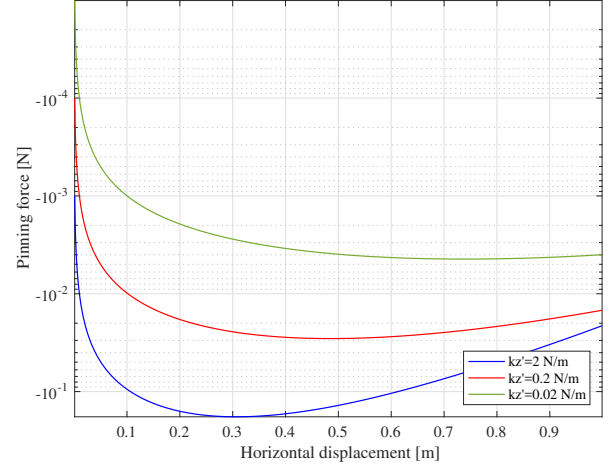


Fig. 10. The horizontal pinning force when the position changes along with x axis

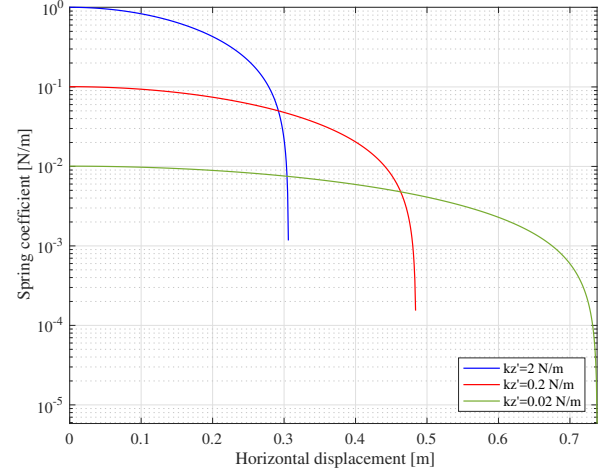


Fig. 11. The horizontal spring coefficient when the position changes along with x axis

Table 1. Parameters for the numerical calculation

Parameters for the space telescope

H_{mis}	6.0 m
R_{mis}	1.9 m
W_{mis}	500 kg
H_{bus}	2.6 m
R_{bus}	1.9 m
W_{bus}	500 kg

Parameters for the PM (NdFeB)

H_{pe}	0.05 m
R_{pe}	0.05 m
m_{pe}	$7.41 \times 10^5 \text{ A/m}^2$

nal points. When the permanent magnet moves beyond a point, the pinning force does not affect between the permanent magnet and the type-II superconductor and then the Meissner effect becomes dominant. The spring coefficient becomes minus when the permanent magnet passes through the final point because of the Meissner effect in this model. This effective range between the initial point and the final point increases when vertical spring coefficient becomes small. However these effective

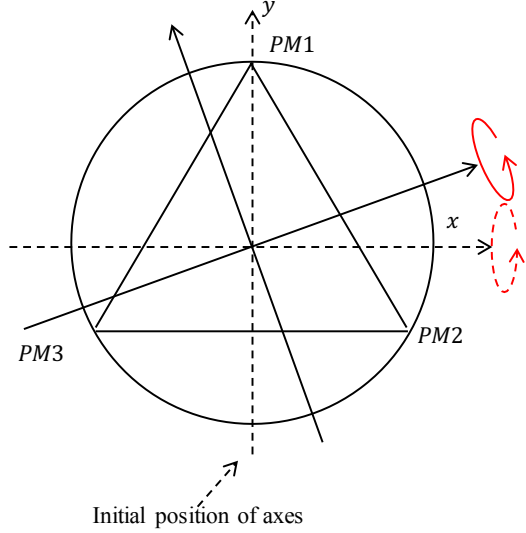


Fig. 12. Rotational coordinate changing with respect to z axis at each angle

ranges may become shorter when a type-II superconductor that is finite size is used for the proposed isolator.

Fig.10 and Fig.11 show horizontal pinning force and spring coefficient. As the horizontal results are compared with the vertical results, the characteristics are different. The gradient of horizontal force with deviation is small compared with that of vertical force, therefore the horizontal spring coefficient is smaller than vertical spring coefficient. However, maximum horizontal force is more bigger than vertical force in every cases. Those characteristics are more outstanding when the pinning force becomes bigger. The relation between horizontal spring coefficient at initial point k'_r and vertical spring coefficient k'_z can be simply expressed as $k'_r \simeq k'_z/2$.

The weak pinning force leads separation accident. As the space telescope that has FMVI changes the attitude, the centrifugal force becomes effective between the mission and bus parts. This force can be much bigger than the pinning force and then causes separation accident. Therefore a system to maintain the relative position forcibly, which use the electro-magnetic coils, is being considered. This system may allow the space telescope not only to maintain the relative position but also to change the observation direction. A type-II superconductor in the superconducting state have the Meissner effect which interrupts external magnetic flux to intrude in the type-II superconductor. This effect creates repulsive force between the type-II superconductor in superconducting state and external magnetic flux. When observation direction change is required, external magnetic flux that is generated by the electro-magnetic coils on the bus part is applied to the type-II superconductor. Observation direction is changed with infinitesimal angle by controlling the external magnetic flux generated by these coils. This is useful when the space telescope is observing a Galaxy or an Exoplanet which are far from the space telescope. Before designing this observation direction change system, characteristic of torque must be understood.

It is considered that the mission part rotates around only x axis to understand the property and the coordinate rotates around z axis as Fig.12. Fig.13 and Fig.14 are the torque prop-

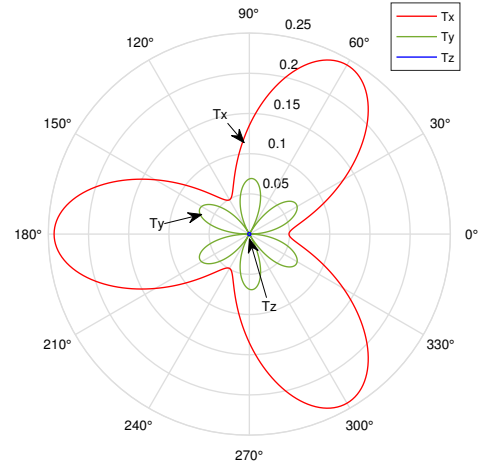


Fig. 13. Torque around an axis on $x - y$ plane with 8 degree

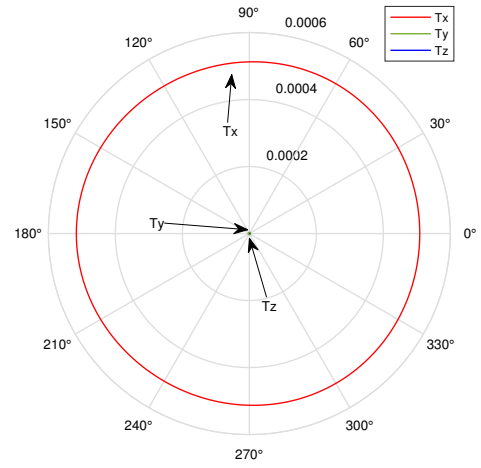


Fig. 14. Torque around an axis on $x - y$ plane with 0.008 degree

erties when the mission part rotates 0.8° and 0.08° in case of $k'_z = 0.02[N/m]$. When the coordinate is at 0° , which is at initial position, the torque is approximately $0.05[Nm]$. At 60° , 180° and 300° maximum torque affects the mission part in Fig.13. In contrast, minimum torque works to the mission part at 0° , 120° and 240° . At these angles, only torque around x axis affects the mission part. The reason why the difference of the pinning force occurs is the Meissner effect. The repulsive force by the Meissner effect is bigger than the pinning force and appears when a permanent magnet approaches to a type-II superconductor in the superconducting state. When the mission part rotates around x axis with counter-clockwise direction at initial position, PM2 and PM3 approach to the type-II superconductors. When rotated coordinate is located on 60° , then PM2 approaches to the bus part. In these cases, the distance between x axis and the permanent magnet which approaches to the type-II superconductor is different. The case of 60° has the distance which is bigger than the case of rotation at initial position. This distance is the biggest in case of 60° , 180° and 300° and be-

come the smallest in case of 0° , 120° and 240° . Therefore the repulsive force of 60° , 180° and 300° become the biggest and the case of 0° , 120° and 240° have the smallest force.

When the mission part rotates around x axis at the others, torque around another axis affects in the proposed isolator as coupling effect. This coupling effect can not be neglected as the mission part rotates with few degree. When the rotational motion of the mission part is considered, this effect have to be considered. However, Fig.14 shows coupling effect can be dealt as small when the mission part rotates with small angle. In the operation of changing observation direction with infinitesimal angle, the effect may be neglected.

6. Conclusion

The micro vibration isolator using the flux pinning effect is proposed and the characteristics are analyzed. Low spring coefficient and adjusted damping coefficient are required to suppress the vibration in broadband passively. The spring coefficient at the initial position depends on the parameters of the type-II superconductor and the magnitude of the external magnetic field, which applies to the type-II superconductor. The pinning force decreases significantly when the low spring coefficient at the initial point is achieved. However the pinning force may maintain the relative distance and attitude between the mission and bus parts even if SRP works to the space telescope. The type-II superconductor is assumed as sufficiently large in the frozen image model. Therefore, if the type-II superconductor is finite size, the pinning force becomes smaller. The force have to be estimated by another numerical model. When the mission part rotates with respect to the bus part, the magnitude difference of the torque and the coupling effect were seen in the numerical result. This effect can be neglected when rotational motion of the mission part with infinitesimal angle is considered. However this properties have to be understood when the mission part rotates with few degrees. As future works, the performance of frequency response have to be confirmed experimentally. And the observation direction change controller will be designed.

References

- 1) Ogawa, H., Nakagawa, T., and et.al.: New cryogenic system of the next-generation infrared astronomy mission SPICA, *Proc. SPIE*, Edinburgh, (2016).
- 2) Lundquist, R. A., Balzano, V. and et.al.: Status of the James Webb Space Telescope integrated science instrument module, *Proc. SPIE*, Amsterdam, (2012).
- 3) Rahman, Z. H., Spanos, J. T. and Laskin, R. A.: A six axis vibration isolation, suppression and steering system for space applications, *Proc. AIAA Dynamics Specialist Conference*, Salt Lake City, (1996), pp.441–449.
- 4) Davis, P. L., Carter, R. D. and Hyde, T. T.: Second generation hybrid D-strut, *Proc. SPIE*, 161, San Diego, (1995).
- 5) McInroy, E. J. and Hamann, C. J.: Design and Control of Flexure Jointed Hexapods, *Trans. Robot. Autom.*, **16**, (2000), pp. 372–381.
- 6) Marneffe, B., Avraam, M. and et. al.: Vibration Isolation of Precision Payloads: A Six-Axis Electromagnetic Relaxation Isolator, *J. Guid. Control Dynam.*, **32**, (2009), pp.395-401.
- 7) Fujiwara, K., Yasuda, S. and et. al.: Accelerometer Assisted High Bandwidth Control of Tip-Tilt Mirror for Precision Pointing Stability, *Proc. IEEE Aero. Conf.*, (2011), Montana, pp.1–7.
- 8) Shimizu, T., Nagata, S. and et. al.: Image Stabilization System for Hinode (Solar-B) Solar Optical Telescope, *J. Sol. Phys.*, **249**, (2008), pp.221–232.
- 9) Pedreiro, N.: Spacecraft Architecture for Disturbance-Free Payload, *J. Guid. Control Dynam.*, **26**, (2003), pp.794-804.
- 10) Shibata, T. and Sakai, S.: Passive Micro Vibration Isolator Utilizing Flux Pinning Effect for Satellites, *J. Phys. Conf. Ser.*, **744**, (2016), 012009.
- 11) Shoer, P. J. and Peck, A. M.: Reconfigurable Spacecraft as Kinematic Mechanism Based on Flux Pinning Interaction, **46**, (2009), pp. 466–469.
- 12) Sorgenfrei, C. M., Jones, L. L. and et. al.: Testbed Validation of Location-Scheduled Control of a Reconfigurable Flux Pinned Spacecraft Formation, *textit{J. Spacecr. Rockets}*, **50**, (2013), pp. 1235–1247.
- 13) Jones, L.L., Wilson, R. W. and et. al: Design Parameters and Validation for a Non-Contacting Flux-Pinned Docking Interface, Anaheim, (2010).
- 14) O'Neil, J. W. and Cazaux, C.: The Mars Sample Return Project, *Acta Astron.*, **47**, (2000), pp.453–465.
- 15) Clark, C. B.: Mars Sample Return: The Critical Next Step, *Acta Astron.*, **61**, (2007), pp.95–100.
- 16) Teshima, H.: Combination of Additional Noncontact Dampers and Superconducting Levitation Using Melt-processed YBaCuO Bulk Superconductors, *Jnp. J. Appl. Phys.*, **36**, (1997), pp.68-75.
- 17) Shoer, P. J. and Peck, A. M.: Flux-Pinned Interfaces for the Assembly, Manipulation, and Reconfiguration of Modular Space Systems, *J. Aerospace Eng.*, **57**, (2009), pp.667–688.
- 18) Kaneda, R., Sakai S. and et. al: The Relative Position Control in Formation Flying Satellites using Super-Conducting Magnets, *Proc. International Symposium on Formation Flying Missions and Technologies*, Washington DC, (2004).
- 19) Kordyuk, A. A.: Magnetic Levitation for Hard Superconductor, *J. Appl. Phys.*, **83**, (1998), pp.610–612.
- 20) Shibata, T. and Sakai, S.: Design Method for The Micro Vibration Isolator Using Flux Pinning Effect for Satellites, *Proc. Astrodynamics Specialist Conference*, Long Beach, (2016).
- 21) Brown, D. C.: Spacecraft Propulsion, *AIAA Education Series*, (1996).